Three-term formulation to describe infiltration in water-repellent soils

Deniz Yilmaz [a,*], Simone Di Prima [b,c], Ryan D. Stewart [d], Majdi R. Abou Najm [e],
David Fernandez-Moret [f], Borja Latorre [f], Laurent Lassabatere [c]

[a] *Civil Engineering Department, Engineering Faculty, Munzur University, Tunceli, Turkey*
[b] *Department of Agricultural Sciences, University of Sassari, Viale Italia, 39A, 07100 Sassari, Italy*
[c] *Université de Lyon, UMR5023 Ecologie des Hydrosystèmes Naturels et Anthropisés, CNRS, ENTPE, Université Lyon 1, Vaulx-en-Velin, France*
[d] *School of Plant and Environmental Sciences, Virginia Polytechnic Institute and State University, Blacksburg, VA, United State*
[e] *Department of Land, Air and Water Resources, University of California, Davis, CA 95616, United States*
[f] *Departamento de Suelo y Agua, Estación Experimental de Aula Dei, Consejo Superior de Investigaciones Científicas (CSIC), PO Box 13034, 50080 Zaragoza, Spain*

ARTICLE INFO	ABSTRACT
	Modeling infiltration in water-repellent soils is difficult, as the underlying processes remain poorly quantified. However, recent work has adapted the Beerkan Soil Transfer Parameter (BEST) algorithm to include an exponential correction term for characterizing these types of soils. The original BEST-WR (WR = Water Repellent) method used a two-term approximate expansion of the Haverkamp quasi-exact implicit model. However, the BEST-WR method can have considerable inaccuracy, particularly as the time of infiltration and the soil water repellency increase. Here, we extended the BEST-WR model by adapting a three-term approximation of the Haverkamp quasi-exact implicit model to water-repellent soils. We then tested the new method using analytical data. For highly water-repellent soils, the proposed method had better performance when estimating soil sorptivity (S) and soil saturated conductivity (K_s), with respective errors of less than 1.5 % and 8 %, compared to relative errors of more than 10 % and 30 % with the two-term BEST-WR method. We also tested both approaches with experimental data. The two methods provided similar estimates for hydraulic parameters, with linear correlations between methods of $R^2 = 0.84$ for S and $R^2 = 0.88$ for K_s. Initial infiltration was not well modeled by either the two-term or three-term model for 33 tests, thus revealing limitations in the applied exponential model that we used to account for soil repellency. Nonetheless, the proposed three-term expression provided better fits than the two-term model for most of the infiltration runs, meaning that this new approach is more robust when modeling infiltration processes in water-repellent soils.

1. Introduction

Infiltration is the process by which water moves into the soil surface. This mechanism is important for recharging soil water and, in some instances, deeper groundwater. Infiltration acts as a primary control on surface runoff and soil erosion, and lower infiltration rates can be therefore be associated with water quality degradation (Gette-Bouvarot et al., 2015; Bouwer, 1999). Many different approaches have been used to describe and model infiltration processes in fully wettable soils, typically considering either one-dimensional vertical (1D) or three-dimensional (3D) flow processes. However, these models tend to perform poorly when applied to water-repellent soils, which are characterized by reduced wettability due to soil particles becoming coated by hydrophobic organic substances that often originate from vegetation

(Cerdà and Doerr, 2007). Specifically, most infiltration models simulate a concave curve for cumulative infiltration versus time, whereas water-repellent soils often have convex or sigmoidal relationships due to increasing soil wettability with time (e.g., Lassabatere et al., 2019; Angulo-Jaramillo et al., 2019; Beatty and Smith, 2013). To address this issue, Abou Najm et al. (2021) proposed an exponential correction term in order to model infiltration rates in water-repellent soils. Those authors combined their correction factor with the simple two-term cumulative infiltration model developed by Haverkamp et al. (1994) as an approximate expansion of their quasi-exact implicit (QEI) model. By doing so, Abou Najm et al. (2021) proposed a new formulation and demonstrated its ability to model a wide range of soil conditions. Based on this initial work, Di Prima et al. (2021) implemented the new formulation into the BEST (Beerkan Soil Transfer Parameter) method,

creating the BEST-WR model (WR = water repellency).

BEST is based on a pair of two-term equations, obtained as approximate expansions of the QEI model, that fit infiltration behaviors at short and long times, thus making the set of equations valid for both transient and steady-state conditions. There are three variations of the BEST method: BEST-Slope (Lassabatere et al., 2006), BEST-Intercept (Yilmaz et al., 2010) and (BEST-steady) (Bagarello et al., 2014). The BEST-Slope and BEST-Intercept methods use both short- and long-time equations, while BEST-steady is based only on long times. The BEST-Slope and BEST-Intercept differ in the constraints that are used to relate sorptivity and saturated conductivity (Angulo-Jaramillo et al., 2019). The robustness of these three methods have been assessed in many studies (e. g., Yilmaz et al., 2019; Di Prima et al., 2019; Castellini et al., 2016), and all are now widely used in the scientific community.

The three BEST variations are designed to model cumulative infiltration curves that are concave in shape, and thus cannot effectively describe the convex shapes often seen in water-repellent soils. Di Prima et al. (2021) coupled the BEST-slope method with the Abou Najm et al. (2021) correction term to create a new two-term model for water-repellent soils. Their model, hereafter called BEST-WR-2T, was verified with analytical and empirical data from hydrophilic (i.e., fully wettable) and water-repellent soils. Overall, this approach worked well, yet the error of estimated values of soil sorptivity (*S*) and saturated hydraulic conductivity (K_s) increased as soils became more water-repellent, leading to questions about the time-scale over which this two-term approach is accurate. In particular, analytical soils with strong water repellency had deviations of up to 30 % between estimated and reference K_s. Previously, Lassabatere et al. (2006) delimited the time over which the two-term equation is valid by ensuring that the infiltration flux at long times does not exceed that of short times. The corrective term proposed by Abou Najm et al. (2021) was designed to fit any infiltration model, but did not specifically consider the validity of specific functions such as the two-term equation adapted to water repellency. In contrast, Di Prima et al (2021) focused their approach to specifically use the transient portion of the two-term equation, and therefore did not investigate the time intervals over which the solution was valid.

Recently, Rahmati et al. (2019) proposed a formulation using a three-term expansion, i.e., the three first terms of series development of the QEI model proposed by Haverkamp et al. (1994). This approximation was shown to be valid for a longer duration than the two-term formulation, since it includes one additional term of the series. Nonetheless, the exact time of validity is not directly calculable, and a comparison procedure must be done with the implicit quasi-exact cumulative infiltration curve to detect the time at which the three-term model begins to deviate. Next, Moret-Fernández et al. (2020) developed a four-term expression for 3D infiltration, and tested it with disk-infiltrometer measurements. Finally, Rahmati et al. (2020) proposed a five-term expansion. The latter two expansions of the QEI formulation are valid for longer times than the other solutions. However, the 4th and 5th terms are expected to have small magnitudes and thus to only increase the precision of the expansions by a small extent relative to the simpler three-term expansion (Moret-Fernández et al., 2020, Rahmati et al., 2020).

In this paper, we couple the Abou Najm et al. (2021) exponential correction term and the three-term expansion (Rahmati et al., 2019) of the Haverkamp model (Haverkamp et al., 1994) to describe more accurately the infiltration process for water-repellent soils over large time intervals. This new formulation, hereafter called BEST-WR-3T, describes 3D infiltration through water-repellent soils and considers both transient and steady-state infiltration, thus addressing a major limitation of BEST-WR-2T. We hypothesized that the BEST-WR-3T model would provide more accurate estimates than the BEST-WR-2T model for three important parameters: soil sorptivity *S*, correction factor α_{WR}, and saturated hydraulic conductivity K_s. For this analysis, we first generated numerical infiltration data for hydrophilic and water-

repellent soils for six synthetic soils. Then we tested the new approach with field data measured in Berchidda, Italy (Di Prima et al., 2021). Finally, we discussed the benefits of BEST-WR-3T compared to BEST-WR-2T model and examined how using longer duration datasets affect estimates of *S* and K_s.

2. Theoretical development

The BEST method was developed first by Lassabatere et al. (2006) to estimate the parameters of the van Genuchten (1980) water retention curve, $\theta(h)$, with the Burdine (1953) condition, and the Brooks and Corey (1964) relationship for hydraulic conductivity, $K(\theta)$:

$$\theta(h) = \theta_s[1 + (\alpha_{vG}|h|)^n]^{-m} \tag{1a}$$

$$m = 1 - \frac{2}{n} \tag{1b}$$

$$K(\theta) = K_s \left(\frac{\theta}{\theta_s}\right)^{\eta} \tag{1c}$$

$$\eta = \frac{2}{nm} + 3 \tag{1d}$$

where *h* (L) is the water pressure head, α_{vG} (L^{-1}) is the van Genuchten pressure scale parameter, K_s (L/T) is the saturated hydraulic conductivity at the soil surface, and θ_s (L^3 L^{-3}) is the saturated soil water content. Note that the case of a null residual soil water content, $\theta_r = 0$, corresponds to the case addressed by BEST methods (Angulo-Jaramillo et al., 2019). The shape parameters *n*, *m* and η are deduced from particle size distribution using specific pedo-transfer functions (PTF). More details on the estimation of these parameters can be found in Lassabatere et al. (2006) or Minasny and McBratney (2007). The K_s and α_{vG} parameters are derived by analyzing water infiltration data.

The 3D cumulative infiltration, *I*(t) (L), and infiltration rate, *i*(t) (L/T), from a circular source for a null pressure head can be approximated by the following two-term (2T) explicit transient expressions (Haverkamp et al., 1994):

$$I_{2T}(t) = S\sqrt{t} + (AS^2 + BK_s)t \tag{2a}$$

$$i_{2T}(t) = \frac{S}{2\sqrt{t}} + (AS^2 + BK_s) \tag{2b}$$

$$B = \frac{2 - \beta}{3} \tag{2c}$$

where *t* (T) is the time elapsed since the start of the infiltration event, *S* (L/T$^{-0.5}$) is the soil sorptivity, and $A = \frac{\gamma}{r(\theta_s - \theta_i)}$ defines an additional part, i.e., $AS^2 t$, that is needed to convert 1D to 3D cumulative infiltration. β and γ are parameters that are often respectively fixed to 0.6 and 0.75 (Angulo-Jaramillo et al., 2019), and θ_i (L^3 L^{-3}) is the initial volumetric soil water content. Note that in Equation (2), we neglect the effect of the initial hydraulic conductivity, K_i, as is commonly done in other studies (e.g., Moret-Fernández et al., 2020). For long-time expansions the cumulative infiltration and infiltration rate are defined as:

$$I_{+\infty}(t) = (AS^2 + K_s)t + \frac{1}{2(1 - \beta)}\ln\left(\frac{1}{\beta}\right)\frac{S^2}{K_s} \tag{2c}$$

$$i_{+\infty} = AS^2 + K_s \tag{2d}$$

For relatively dry soil conditions, where $K_i \cong 0$, Rahmati et al. (2019) developed a series expansion for short-time cumulative infiltration, leading to the three-term expansion below:

$$I_{3T}(t) = I_{2T}(t) + \frac{1}{9}(\beta^2 - \beta + 1)\frac{K_s^2}{S}t^{\frac{3}{2}} \tag{3a}$$

Table 1

Soil hydraulic parameters of the van Genuchten-Mualem (vGM) model for the six studied soils used to model the infiltration experiments. Values came from the Carsel and Parrish (1988) database.

Soil texture	Sand	Loamy Sand	Sandy Loam	Loam	Silt Loam	Silty Clay Loam
θ_r	0.045	0.057	0.065	0.078	0.067	0.089
θ_i	0.083	0.092	0.100	0.113	0.105	0.123
θ_s	0.43	0.41	0.41	0.43	0.45	0.43
α_{VG} (mm^{-1})	0.0145	0.0124	0.0075	0.0036	0.002	0.001
n	2.68	2.28	1.89	1.56	1.41	1.23
K_s (mm h^{-1})	297.0	145.9	44.2	10.44	4.5	0.7
S (mm h$^{-0.5}$)	86.5	58.2	36.0	20.9	16.3	6.0
l	0.5	0.5	0.5	0.5	0.5	0.5

Where θ_i is the initial volumetric water content, α_{VG} and n correspond to the water retention curve of the vGM model and l is the tortuosity parameter.

The corresponding infiltration rate is:

$$i_{3T}(t) = i_{2T}(t) + \frac{1}{6}\left(\beta^2 - \beta + 1\right)\frac{K_s^2}{S}t^{\frac{1}{2}} \tag{3b}$$

At long times, the measurement of the infiltration rate asymptote, $i_{+\infty}^{exp}$ (Equation 2d), allows K_s to be linked to S as follows (Lassabatere et al., 2006):

$$K_s = i_{+\infty}^{exp} - AS^2 \tag{4}$$

Introduction of Equation (4) into the two-term (2T) and three-term (3T) formulations allows us to rewrite the cumulative infiltration and infiltration rate equations as follows:

$$I_{2T}(t) = S\sqrt{t} + \left[A(1-B)S^2 + Bi_{+\infty}^{exp}\right]t \tag{5a}$$

$$i_{2T}(t) = \frac{S}{2\sqrt{t}} + \left[A(1-B)S^2 + Bi_{+\infty}^{exp}\right] \tag{5b}$$

$$I_{3T}(t) = I_{2T}(t) + \frac{1}{9}\left(\beta^2 - \beta + 1\right)\frac{\left(i_{+\infty}^{exp} - AS^2\right)^2}{S}t^{\frac{3}{2}} \tag{5c}$$

$$i_{3T}(t) = i_{2T}(t) + \frac{1}{6}\left(\beta^2 - \beta + 1\right)\frac{\left(i_{+\infty}^{exp} - AS^2\right)^2}{S}t^{\frac{1}{2}} \tag{5d}$$

Abou Najm et al. (2021) proposed the following correction factor to describe infiltration rate into water-repellent soils, $i_{WR}(t)$:

$$i_{WR}(t) = i(t)(1 - e^{-\alpha_{WR}t}) \tag{6}$$

in which α_{WR} (T^{-1}) is an empirical parameter considered to reflect the rate of water repellency attenuation during infiltration.

Di Prima et al. (2021) used this factor, along with Equation (5a) and (5b), to obtain the BEST-WR-2T formulation:

$$i_{WR2T}(t) = \left\{\frac{S}{2\sqrt{t}} + \left[A(1-B)S^2 + Bi_{+\infty}^{exp}\right]\right\}(1 - e^{-\alpha_{WR}t}) \tag{7a}$$

$$I_{WR2T}(t) = S\sqrt{t} - \frac{S\sqrt{\pi}}{2\sqrt{\alpha_{WR}}}erf\left(\sqrt{\alpha_{WR}t}\right) + \left[A(1-B)S^2 + Bi_{+\infty}^{exp}\right]t - \frac{\left[A(1-B)S^2 + Bi_{+\infty}^{exp}\right](1 - e^{-\alpha_{WR}t})}{\alpha_{WR}} \tag{7b}$$

where $i_{WR2T}(t)$ is the adapted two-term infiltration rate with water repellency, $i_{2T}(t)$ is the original two-term infiltration rate that does not account for water repellency, and *erf* is the error function.

By analogy to the work of Di Prima et al. (2021), the correction factor for water-repellent soils can be applied to the Rahmati et al. (2019) three-term formulation to obtain the BEST-WR-3T model (see appendices for more details):

$$i_{WR3T}(t) = i_{WR2T}(t) + \frac{1}{6}\left(\beta^2 - \beta + 1\right)\frac{\left(i_{+\infty}^{exp} - AS^2\right)^2}{S}t^{\frac{1}{2}}(1 - e^{-\alpha_{WR}t}) \tag{8a}$$

$$I_{WR3T}(t) = I_{WR2T}(t) + \frac{1}{9}\left(\beta^2 - \beta + 1\right)\frac{\left(i_{+\infty}^{exp} - AS^2\right)^2}{S}t^{\frac{3}{2}}$$
$$- \frac{\left(\beta^2 - \beta + 1\right)}{6}\frac{\left(i_{+\infty}^{exp} - AS^2\right)^2}{S}\left\{-\frac{t^{\frac{1}{2}}}{\alpha_{WR}}e^{-\alpha_{WR}t} + \frac{\sqrt{\pi}}{2(\alpha_{WR})^{\frac{3}{2}}}erf\left(\sqrt{\alpha_{WR}t}\right)\right\} \tag{8b}$$

3. Material and methods

3.1. Analytical data set

The BEST-WR-3T model was verified using synthetic data generated from the hydraulic properties of six conventional soils (Table 1). Three-dimensional infiltration was simulated, and the soils were all assumed to have an initial saturation degree of $S_{e,I} = 0.1$. The procedure for generating water-repellent synthetic infiltration data was based on the extension of the QEI formulation with the correction factor proposed by Abou Najm (2021), as detailed in Di Prima et al. (2021). The α_{WR} parameter varied from 0.04 to 10000 h^{-1} depending on the type of soil (Table 2). The resulting curves covered a range of shapes, from regular concave to convex or with an inflection point. More detailed information about the criteria used to select the α_{WR} parameter values can be found in Di Prima et al. (2021).

3.2. Experimental site

Di Prima et al. (2021) evaluated the BEST-WR-2T model with measurements from the Berchidda site (40°48′57.28 "N, 9°17′33.09 "E), located in the Long-Term Observatory of Berchidda-Monti (NE Sardinia, Italy). For our study, we used the same dataset.

The mean annual temperature at the Berchidda site is 14.2 °C and the mean cumulative precipitation is 623 mm. The place is a Mediterranean wooded meadow with herbaceous species and oaks. The experimental site has two types of land cover: open spaces (grasslands) and tree canopies (Seddaiu et al., 2018). According to the USDA standards, the texture of the soil upper horizon ranged from sandy loam to loamy sand. More details about the soil properties can be found in Di Prima et al. (2021). Di Prima et al. (2021) performed water drop penetration time tests (Wessel, 1988) in the grasslands, and found that the soil surface was wettable in 47.8 % of tested locations, slightly water-repellent in 41.1 % of tested locations, and strongly water-repellent in 11.1 % of tested locations (N = 30). Different water drop penetration time distributions were measured under tree canopies, with 0.0 % of locations determined to be wettable, 4.4 % to be slightly, 27.8 % to be strongly, 46.7 % to be severely, and 21.1 % to be extremely soil water repellent (N = 30). For more details, refer to Di Prima et al. (2021).

3.3. Beerkan experiments

The Beerkan infiltration tests were conducted using automated infiltrometers (Di Prima et al., 2016, Concialdi et al., 2020). A total of 60 Beerkan tests were conducted, with 30 done in open grassland areas and

Table 2
Summary of the soil hydraulic properties estimated for the six synthetic soils. i_s^{exp} and b_s^{exp} respectively correspond to infiltration rate (Equation 4) and the intercept asymptote.

| Soil	α_{WR} (h⁻¹)	i_s^{exp} (mm h⁻¹)	b_s^{exp} (mm)	BEST-WR-3T (Eq. 8b) α_{WR} (h⁻¹)	BEST-WR-2T (Eq. 7b) S (mm h⁻⁰·⁵)	BEST-Slope (Eq. 2a) K_s (mm h⁻¹)	α_{WR} (h⁻¹)	S (mm h⁻¹)	K_s (mm h⁻¹)	S (mm h⁻⁰·⁵)	K_s (mm h⁻¹)
Sand	No WR	523.99	13.5	2.80E+16	85.6	312.76	13,627	91.1	284.88	88.7	297.94
	10,000	523.97	12.7	12,408	85.3	314.19	3283	91.1	284.82	85.8	311.80
	1000	523.97	10.8	1043	85.3	314.20	720	91.2	284.50	73.0	370.58
	800	523.97	10.4	829	85.3	314.22	600	91.2	284.28	67.1	394.37
	600	523.97	9.8	618	85.3	314.27	471	91.3	283.89	55.7	434.58
	400	523.97	8.8	409	85.3	314.36	330	91.4	283.08	47.5	458.96
	200	523.49	6.4	202	85.3	313.70	174	92.1	279.03	30.1	497.43
	100	523.49	2.3	101	85.3	314.03	90	93.0	274.38	11.6	519.61
	80	523.48	0.5	81	85.2	314.17	73	93.4	271.92	6.2	522.35
	60	522.92	−2.3	60	85.3	313.06	54	94.4	265.98	0.1	522.92
	40	521.94	−7.5	40	85.5	311.17	36	96.0	256.50	−7.1	520.51
Loamy sand	No WR	258.07	12.5	9.80E+15	57.6	153.62	7297	61.3	139.89	59.7	145.94
	5000	257.85	11.7	6159	57.4	154.22	1696	61.3	139.76	57.7	153.25
	500	257.85	9.8	521	57.4	154.23	365	61.3	139.58	47.7	186.40
	400	257.88	9.5	414	57.4	154.24	303	61.4	139.46	44.6	195.22
	300	257.88	8.9	308	57.4	154.27	238	61.4	139.25	36.7	215.48
	200	257.88	8.0	204	57.4	154.32	166	61.5	138.83	31.0	227.61
	100	257.64	5.6	101	57.4	153.99	87	62.0	136.77	19.1	246.16
	50	257.64	1.7	50	57.4	154.17	45	62.6	134.33	6.8	256.20
	40	257.63	−0.1	40	57.3	154.23	36	62.9	133.02	3.2	257.30
	30	257.33	−2.8	30	57.4	153.61	27	63.7	129.90	−0.8	257.31
	20	256.60	−7.8	20	57.6	152.09	18	64.8	124.69	−5.4	255.68
Sandy loam	No WR	87.71	15.7	2.40E+15	35.7	46.71	2316	37.6	42.18	36.8	43.98
	1000	87.75	14.6	1202	35.5	46.99	414	37.6	42.18	35.5	47.12
	100	87.67	12.0	103	35.6	46.86	77	37.7	41.82	27.0	64.14
	80	87.67	11.4	82	35.6	46.87	64	37.7	41.77	23.9	69.31
	60	87.67	10.6	61	35.6	46.88	50	37.8	41.69	21.6	72.68
	40	87.67	9.1	41	35.6	46.90	34	37.8	41.53	17.7	77.60
	20	87.67	5.4	20	35.5	46.94	18	38.0	41.07	9.8	84.59
	10	87.60	−0.7	10	35.5	46.85	9	38.5	39.85	2.0	87.47
	8	87.58	−3.5	8	35.5	46.85	7	38.7	39.32	−0.1	87.58
	6	87.53	−7.9	6	35.5	46.78	6	39.0	38.46	−2.6	87.32
	4	86.41	−14.7	4	36.5	43.49	4	40.0	34.77	−5.2	85.54
Loam	No WR	24.57	22.2	4.10E+14	20.7	11.08	520	21.6	9.88	21.3	10.30
	100	24.52	20.2	112	20.6	11.12	56	21.6	9.86	20.3	11.50
	10	24.50	14.6	10	20.6	11.09	9	21.6	9.74	12.8	19.30
	8	24.50	13.5	8	20.6	11.09	7	21.6	9.72	11.6	20.23
	6	24.50	11.7	6	20.6	11.10	5	21.7	9.69	9.9	21.42
	4	24.50	8.4	4	20.6	11.11	4	21.7	9.62	7.1	22.91
	2	24.48	−0.1	2	20.6	11.08	2	21.9	9.36	2.1	24.34
	1	24.45	−14.9	1	20.6	11.05	1	22.2	8.92	−2.1	24.31
	0.8	24.30	−20.7	0.8	20.8	10.69	0.8	22.4	8.53	−3.2	23.99
Silt loam	No WR	12.41	31.1	1.50E+15	16.2	4.82	209	16.8	4.27	16.6	4.44
	80	12.41	29.6	99.2	16.1	4.85	33.5	16.8	4.25	16.3	4.75
	8	12.41	25.0	8.3	16.1	4.85	6.4	16.8	4.24	14.0	6.72
	6.4	12.41	24.1	6.6	16.2	4.84	5.2	16.8	4.23	12.6	7.84
	4.8	12.41	22.7	4.9	16.2	4.84	4.1	16.8	4.23	11.8	8.38
	3.2	12.40	20.2	3.3	16.2	4.84	2.8	16.8	4.21	10.4	9.26
	1.6	12.41	13.7	1.6	16.1	4.85	1.5	16.8	4.19	7.2	10.92
	0.80	12.40	2.9	0.81	16.1	4.85	0.75	16.9	4.10	3.0	12.13
	0.64	12.40	−2.1	0.64	16.2	4.83	0.60	17.0	4.04	1.7	12.31
	0.48	12.39	−10.1	0.48	16.2	4.83	0.46	17.0	3.99	0.0	12.39
	0.32	12.38	−25.1	0.32	16.2	4.82	0.30	17.1	3.86	−2.1	12.26
Silty clay loam	No WR	1.890	27.0	1.40E+13	5.9	0.747	35	6.1	0.661	6.1	0.688
	10	1.896	25.1	11.6	5.9	0.755	4.7	6.2	0.662	5.9	0.756
	1.0	1.896	20.2	1.0	5.9	0.754	0.8	6.2	0.660	4.5	1.249
	0.8	1.896	19.2	0.8	5.9	0.754	0.7	6.2	0.660	4.2	1.316
	0.6	1.895	17.7	0.6	5.9	0.754	0.5	6.2	0.658	3.9	1.412
	0.4	1.895	14.9	0.4	5.9	0.755	0.4	6.2	0.656	3.2	1.557
	0.2	1.896	7.5	0.2	5.9	0.756	0.2	6.2	0.649	1.8	1.787
	0.10	1.894	−4.8	0.10	5.9	0.756	0.09	6.2	0.629	0.3	1.891
	0.08	1.894	−10.6	0.08	5.9	0.755	0.08	6.3	0.620	−0.1	1.893
	0.06	1.893	−19.8	0.06	5.9	0.750	0.06	6.3	0.604	−0.7	1.878
	0.04	1.873	−34.5	0.04	6.0	0.696	0.04	6.4	0.547	−1.3	1.821
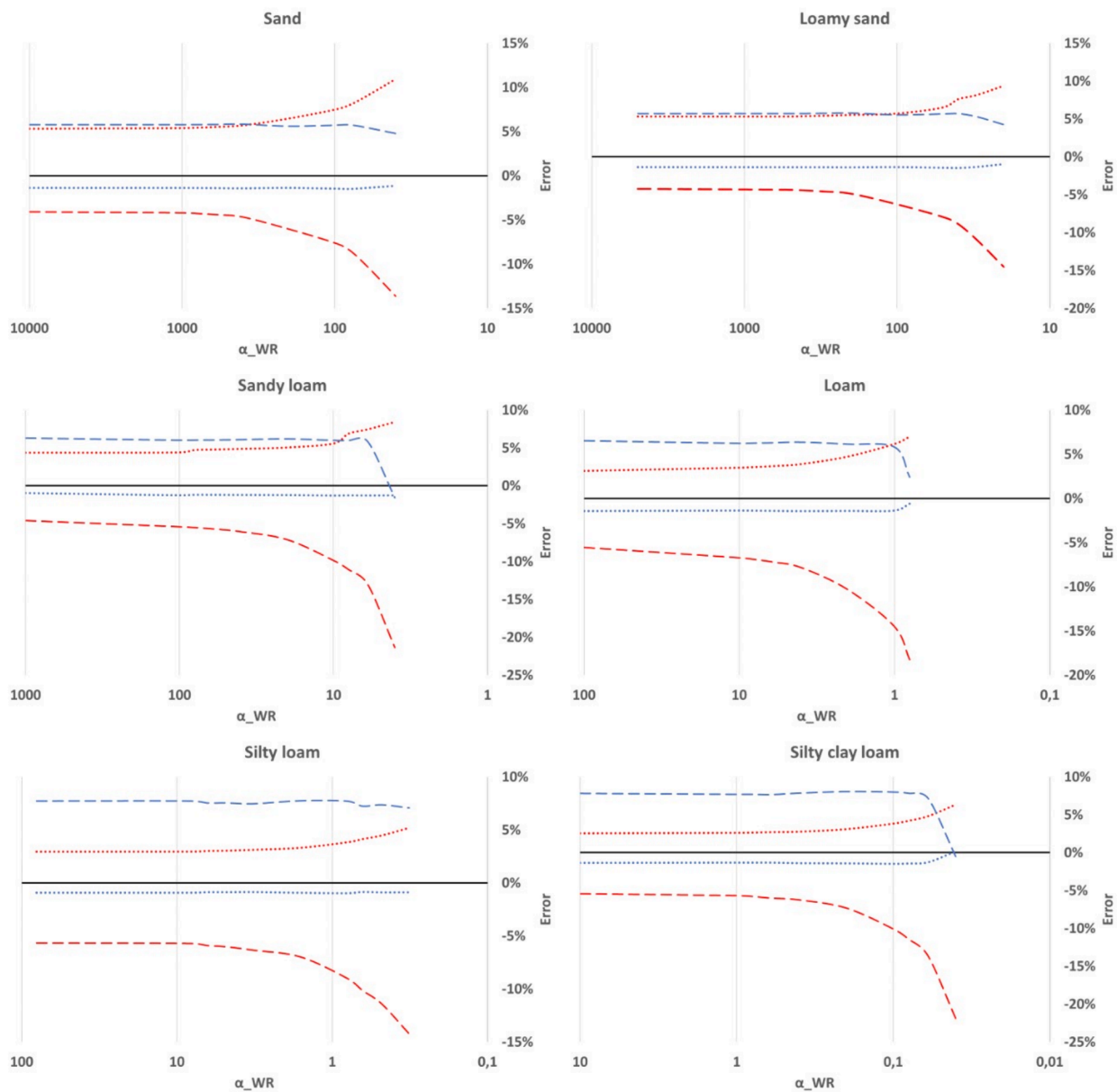
Fig. 1. Error of S [dotted line] and K_s [dashed line] estimates with the respective target value for six synthetic soils, BEST-WR-2T [red line] and BEST-WR-3T [blue line], α_WR [h-1] in horizontal axis and Er [%] in vertical axis.

Table 3
Steady-state time (t_s) and time to which the the two-term (2T) and three-term (3T) expansions first show a 2 % divergence from the QEI formulation for the six synthetic soils.

	QEI	2T	3T
Soil texture	Steady Time [h]	Time to 2 % Divergence [h]	
Sand	0.46	0.04	1.68
Loamy Sand	0.78	0.06	3.16
Sandy Loam	2.69	0.29	13.70
Loam	12.31	2.08	88.21
Silt Loam	33.29	7.98	307.46
Silty Clay Loam	108.60	44.05	1712.00

30 under the tree canopy. The diameter of the infiltration ring was 15 cm, corresponding to an area of 176.7 cm^2. The ring was inserted about 1 cm to avoid surface runoff (Lassabatere et al., 2006). For each Beerkan test a total of 280 mm of water height was infiltrated. Before starting the

infiltration, a plastic film was placed on the soil surface to prevent water infiltration. The data was acquired automatically when the plastic film was removed. The infiltrometers were equipped with differential pressure transducers to measure the water height in the reservoirs. The automated procedure proposed by Concialdi et al. (2020) to treat the transducer output was subsequently applied to determine the cumulative infiltration curves. This procedure uses an algorithm, implemented with the open-source software Scilab (Campbell et al., 2010), that minimizes the effect of tension fluctuations caused by air bubble formation in the Mariotte system. The code can be downloaded from the website bestsoilhydro.net (https://bestsoilhydro.net/infiltrometer/), in the section entitled "automatic treatment of the raw data".

3.4. Detection of steady-state conditions and infiltration curve asymptote

The criterion suggested by Bagarello et al. (1999) was used to separate the infiltration data into transient and steady-state conditions. This procedure consisted of a linear regression analysis for the last three
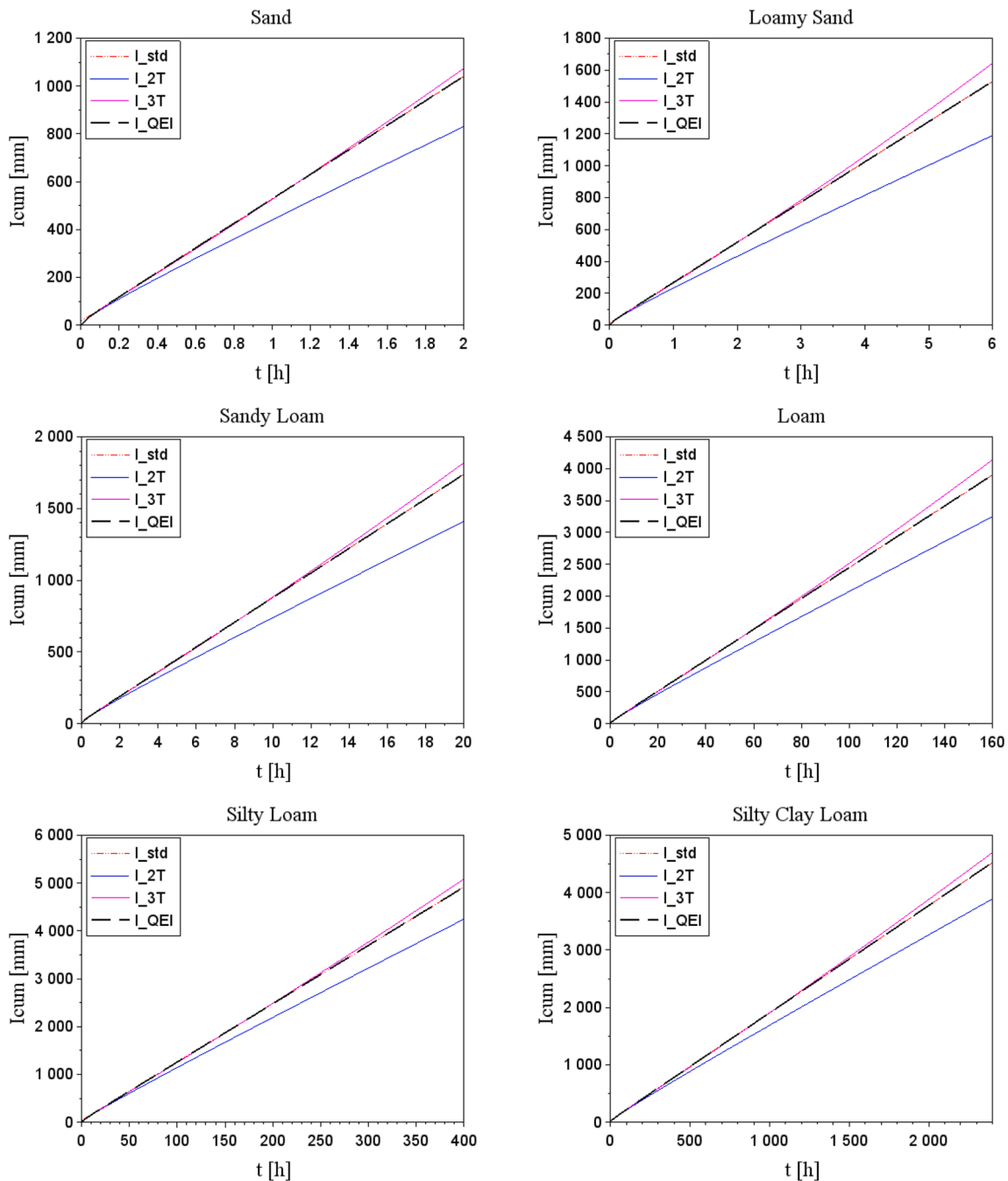
Fig. 2. Cumulative Beerkan curves for the six synthetic soils without repellent effect.

data points of $I(t)$ versus t. Then, the steady-state time (t_s) was determined as the first value for which the following condition was met:

$$\widehat{E} = \left| \frac{I(t) - I_{reg}(t)}{I(t)} \right| \leq E \qquad (9)$$

where $I_{reg}(t)$ is estimated from regression analysis of the last part of the curve, and E defines a given threshold to check linearity. Equation (9) was applied from the end of the experiment until the first data point for which the $\widehat{E} \leq E$ condition was achieved (Angulo-Jaramillo et al., 2016). We adopted the commonly used value of $E = 2$ %. The asymptotic slope, $i_{+\infty}^{exp}$ (L/T), was estimated by linear regression analysis of steady-state data (i.e., all data points measured after the time t_s, when $\widehat{E} \leq 2$).

3.5. Analytical data set used for the inverse procedure

The two-term and three-term expansions are approximations of cumulative infiltration as simulated by the QEI model (Haverkamp et al., 1994). They are valid only for a certain time period, after which time they deviate from the target model. The validity of the two-term transient model is fixed by the following condition (Lassabatere et al., 2006): $t_{valid} < \frac{1}{4(1-B)^2} \frac{S^2}{K_s^2}$. For the three-term formulation, there is no equivalent analytical formulation delimiting the validity of the model. However, Rahmati et al (2019) used a recursive procedure to delimit the time validity of the expansion formulation. In our study, we used a threshold of 2 %, which reflects the percentage of divergence between the QEI cumulated formulation and the corresponding 3T expansion. We first calculated t_s for the six synthetic soils according to criterion of Equation
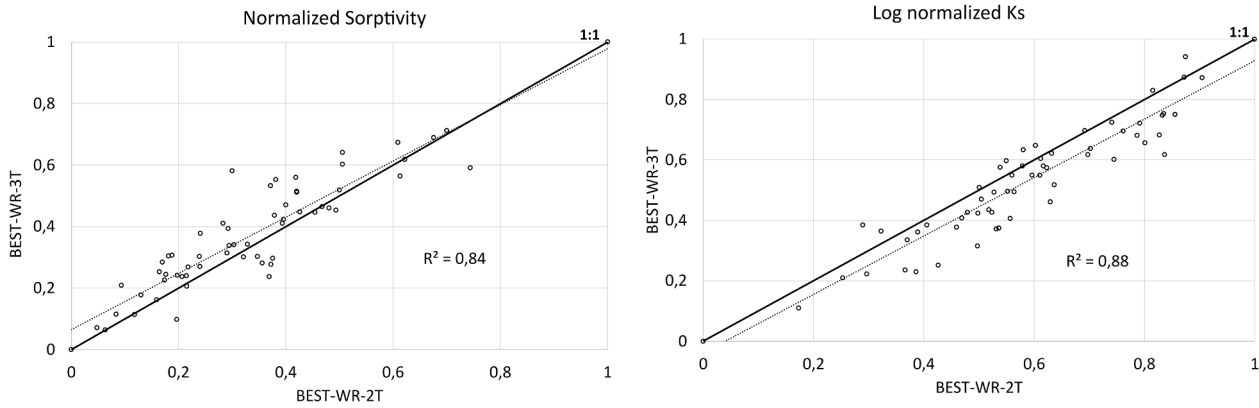
Fig. 3. Plot of normalized S and log normalized K_s estimates from BEST-WR-2T (Di Prima et al. 2021) and BEST-WR-3T (this study).

(9). Then, we compared this value with the divergence time of each formulation for the six synthetic soils.

3.6. Validation of the three-term formulation

A specific program to process the cumulative infiltration curves was developed using Scilab (Campbell et al., 2010). The program first detects the steady state and measures the slope of the asymptote at long times, $i_{+\infty}^{exp}$. We used the inverse function "lsrqsolve" implemented in Scilab (Di Prima et al., 2021) to estimate S and α_{WR} by fitting 1) the BEST-WR-2T model (Equation 7b) to the experimental data corresponding to the transient state and 2) the BEST-WR-3T model (Equation 8b) to the full data set. Note that in this approach we assumed that the BEST-WR-3T model was valid at for times. Finally, we calculated K_s using Equation (4) for both formulations.

We compared the ability of the two models to estimate hydraulic properties from the synthetic infiltration curves by calculating the relative error, Er, for each estimated value of $\widehat{\alpha}_{WR}$, soil sorptivity ($\widehat{S}_{WR}$ and $\widehat{S}$) and saturated soil hydraulic conductivity ($\widehat{K}_{s,WR}$ and $\widehat{K}_s$) as compared to the corresponding reference value:

$$Er(x) = \frac{\widehat{x} - x}{x} \tag{10}$$

where $\widehat{x}$ is the estimated value and x is the target, i.e., the reference values of α_{WR}, S and K_s (Table 1).

For the field data, S and K_s values estimated with BEST-WR-3T were compared to the corresponding values obtained by BEST-WR-2T. To this end, S estimates from both approaches were normalized between 0 and 1 and represented with a regression line to estimate the R^2 factor. As K_s is typically lognormally distributed, we log-normalized K_s (between 0 and 1) to estimate R^2. The accuracy of each model was assessed on the basis of the consistency of the model shape and the relative error of the model fit, Er_{FIT}, which was estimated as follows:

$$Er_{FIT} = \sqrt{\frac{\sum\limits_{i=1}^{k}\left[I_{exp}(t_i) - I_{est}(t_i)\right]^2}{\sum\limits_{i=1}^{k}I_{exp}^2(t_i)}} \tag{11}$$

4. Results and discussion

4.1. Analytical validation for six synthetic soils

The synthetic soils were analyzed using the BEST-Slope (Equation 2a), BEST-WR-2T (Equation 7b), and BEST-WR-3T (Equation 8b) methods, with results reported in Table 2. For non-repellent synthetic soils, the new BEST-WR-3T method yielded very high estimates for the

$\widehat{\alpha}_{WR}$ correction coefficient (in line with the Abou Najm et al. (2021) definition) in comparison to the BEST-WR-2T method. High values of $\widehat{\alpha}_{WR}$ correspond to a scaling factor value of near-unity, which removes the corrective effect of this term and can be interpreted as an indicator of wettable (i.e., non-repellent) soils. When $\widehat{\alpha}_{WR}$ was estimated for water-repellent soils, the three-term approach systematically gave estimates closer to the target value used in the simulations, whereas the BEST-WR-2T algorithm was less precise (Table 2). Better estimation of the $\widehat{\alpha}_{WR}$ parameter translates to better estimations of S, since these two parameters are evaluated simultaneously. This effect is observed by comparing relative errors for S: the BEST-WR-3T model had relative errors that were consistently lower than 1.5 % (Fig. 1), whereas BEST-WR-2T approach provided Er values that were higher and that increased to over 10 % as soils became more water-repellent (i.e., as α_{WR} became smaller).

The BEST-Slope method worked well to estimate S for soils with little water repellency, with relative errors of less than 30 %. However, when the BEST-Slope algorithm was applied to the more repellent soils, the magnitude of estimated S decreased, and in some instances became negative, which is physically implausible. Conversely, the BEST-slope method often provided over-estimates for K_s in the water-repellent soils, as indicated by the relationship in Equation 4. These results clearly show that the BEST-Slope method is not suited for water- repellent soils. However, the BEST-WR-2T method also presented errors when estimating the K_s parameter, with relative differences ranging from 5 % for wettable, non-repellent soils to 25 % when used for severely water-repellent soils. The proposed BEST-WR-3T method resulted in a constant estimate regardless of the soil water repellency (Fig. 1), with errors varying from 5 to 8 %. Therefore, the new BEST-WR-3T approach was more accurate than its two-term counterpart when estimating K_s in soils with severe water repellency.

Table 3 summarizes the estimates of t_s (time for steady-state flow; Equation 9) and the divergence time of the two and three terms expansions versus the QEI formulation for the six synthetic hydrophilic soils. The comparison of deviation times shows that the three-term formulation is valid (and overlapping with the QEI formulation) for much longer than the 2T approach (Fig. 2). Further, the BEST-WR-3T model only diverged from the QEI formulation for t greater than $4t_s$, whereas the BEST-WR-2T term diverged from the QEI formulation within the first hour for the sand and loamy sand soils. These results show that the three-term formulation was suitable for the complete dataset, whereas caution should be taken when using the two-term expansion. We note that, in contrast to the BEST-Slope and BEST-Intercept methods, BEST-WR-2T and BEST-WR-3T approaches do not have specific algorithms to ensure the time-validity of experimental data. Rather, in both approaches, all data points assigned to the transient state are used. This situation may lead to inappropriate fitting if t_s is inappropriately selected. However, the risk of inappropriate fitting is

Table 4
Er$_{FIT}$ calculation, "+" sign is used to indicate the presence of a convex shape for i(t) and a deviation between the BEST-WR-3T model and the experimental data in the initial infiltration phase.

Method BEST	αWR_2T [s^{-1}]	αWR_3T	Er$_{FIT}$ WR-2T	WR-3T	Convex i(t) Shape	Initial Deviation
Berchidda_1F_1	0.0016	0.0010	0.026	0.031		+
Berchidda_1F_2	0.0004	0.0003	0.018	0.023	+	+
Berchidda_1F_3	0.0499	0.0401	0.015	0.008		
Berchidda_1F_4	0.0544	0.0664	0.008	0.005		
Berchidda_1F_5	0.0025	0.0019	0.021	0.020		
Berchidda_1F_6	0.0153	0.0162	0.012	0.005		
Berchidda_1F_7	0.0034	0.0021	0.019	0.021		+
Berchidda_1F_8	0.0098	0.0147	0.020	0.011		
Berchidda_1F_9	0.3773	2.10E+11	0.009	0.019		
Berchidda_1F_10	0.0388	0.1041	0.006	0.013		
Berchidda_1S_1	0.0018	0.0014	0.029	0.034	+	+
Berchidda_1S_2	0.0103	0.0063	0.027	0.015	+	
Berchidda_1S_3	0.0018	0.0015	0.030	0.027	+	+
Berchidda_1S_4	0.0021	0.0018	0.019	0.022		+
Berchidda_1S_5_	0.0008	0.0006	0.031	0.015		
Berchidda_1S_6	0.0041	0.0020	0.029	0.059	+	+
Berchidda_1S_7	0.0883	0.4893	0.005	0.004		
Berchidda_1S_8	0.0006	0.0005	0.032	0.019	+	+
Berchidda_1S_9	0.0010	0.0010	0.023	0.020	+	+
Berchidda_1S_10	0.0022	0.0014	0.032	0.032	+	+
Berchidda_2F_1	0.0439	0.0162	0.017	0.020	+	+
Berchidda_2F_2	0.0290	0.0217	0.023	0.022		
Berchidda_2F_3	0.0013	0.0008	0.023	0.041		+
Berchidda_2F_4	0.0013	0.0007	0.027	0.042		+
Berchidda_2F_5	0.0016	0.0008	0.045	0.061	+	+
Berchidda_2F_6	0.0017	0.0013	0.024	0.026		+
Berchidda_2F_7	0.1947	0.4743	0.005	0.006		
Berchidda_2F_8	0.0020	0.0012	0.025	0.034	+	+
Berchidda_2F_9	0.0071	0.0035	0.018	0.029	+	+
Berchidda_2F_10	0.0034	0.0021	0.032	0.043	+	+
Berchidda_2S_1	0.0057	0.0030	0.033	0.037	+	+
Berchidda_2S_2	0.0026	0.0014	0.029	0.043		+
Berchidda_2S_3	0.0285	0.0342	0.008	0.005		
Berchidda_2S_4	0.0028	0.0015	0.022	0.026		+
Berchidda_2S_5	0.0017	0.0014	0.025	0.022		+
Berchidda_2S_6	0.0014	0.0011	0.026	0.024		
Berchidda_2S_7	0.0010	0.0009	0.017	0.013		
Berchidda_2S_8	0.0029	0.0016	0.031	0.019	+	+
Berchidda_2S_9	0.0030	0.0035	0.014	0.006		
Berchidda_2S_10	0.0020	0.0013	0.019	0.026	+	+
Berchidda_3F_1	0.0192	0.0114	0.026	0.015		
Berchidda_3F_2	0.0038	0.0016	0.036	0.041	+	+
Berchidda_3F_3	0.0008	0.0004	0.027	0.040		+
Berchidda_3F_4	0.0036	0.0020	0.019	0.040	+	+
Berchidda_3F_5_	0.0859	0.0099	0.008	0.022	+	+
Berchidda_3F_6	0.0004	0.0003	0.036	0.037	+	+
Berchidda_3F_7	0.0011	0.0006	0.035	0.043	+	+
Berchidda_3F_8	0.0006	0.0006	0.013	0.012		
Berchidda_3F_9	0.0016	0.0010	0.021	0.027		+
Berchidda_3F_10	0.0202	0.0334	0.013	0.003		
Berchidda_3S_1	0.0025	0.0009	0.035	0.066		+
Berchidda_3S_2	0.0010	0.0006	0.024	0.046		+
Berchidda_3S_3_	0.0002	0.0002	0.016	0.016		
Berchidda_3S_4	0.0002	0.0002	0.022	0.018	+	+
Berchidda_3S_5	0.0018	0.0014	0.021	0.030		
Berchidda_3S_6	0.0005	0.0004	0.028	0.026	+	+
Berchidda_3S_7	0.0004	0.0003	0.049	0.048	+	+
Berchidda_3S_8	0.0098	0.0173	0.027	0.008		
Berchidda_3S_9	0.0008	0.0008	0.008	0.009		
Berchidda_3S_10	0.0013	0.0009	0.021	0.032		+

less important for BEST-WR-3T since the model used for the fit is expected to be accurate for a larger time interval (4t_s instead of t_s).

4.2. Experimental assessment of the proposed three-term formulation

Based on 60 experimental infiltration tests, the BEST-WR-2T and BEST-WR-3T methods provided consistent estimates for hydraulic properties (Fig. 3). Comparing parameter values from the two methods showed R^2 values of 0.84 for normalized S and 0.88 for normalized log

(K_s). Parameter magnitudes varied between methods, however, with BEST-WR-2T generally detecting higher normalized log(K_s) values than BEST-WR-3T. The maximum relative difference was 66 %. When estimating S, however, neither method showed a bias towards over- or under-estimates. The absolute relative difference for the BEST-WR-3T model was less than 20 % for 94 % of the cases, and the maximum relative difference observed was 30 %.

The Er$_{FIT}$ model accuracy indicator (i.e., Equation 11) showed that BEST-WR-2T was better for 33 infiltration tests, versus 27 infiltration
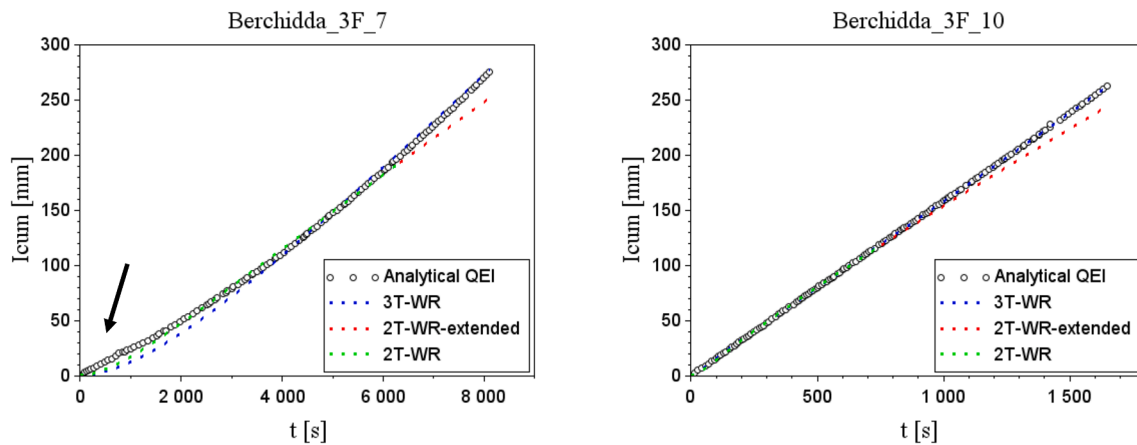
Fig. 4. Example of experimental cumulated infiltration curves and respective BEST-WR-2T (red) and BEST-WR-3T (Blue) models with non-perfect (left) and perfect fitting (right).
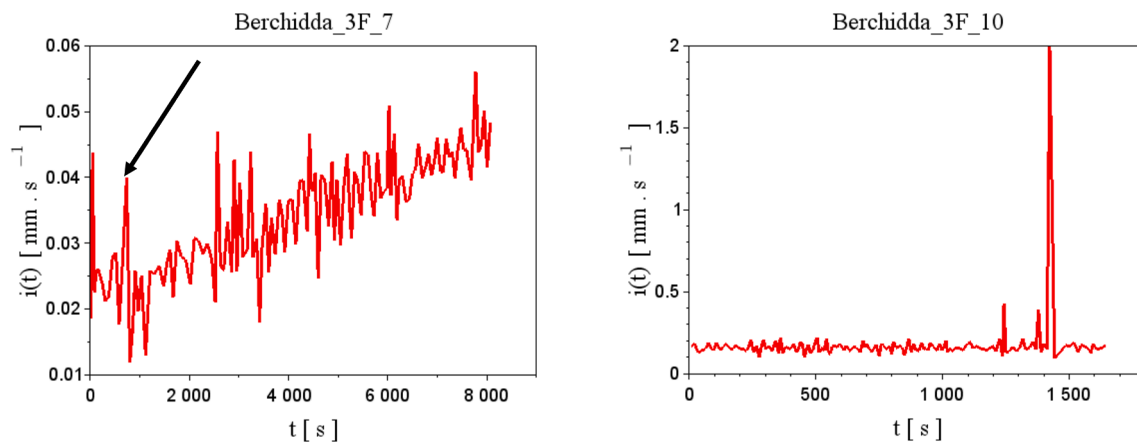

Fig. 5. Example of experimental infiltration rate curves, water repellent behavior marked with a convex shape (left) and linear shape (right).

tests in which the BEST-WR-3T formulation presented better accuracy (Table 4). However, both models often showed deviations from the measured infiltration rates for early time (example shown in Fig. 4, left). For BEST-WR-3T model, this gap was observed in 37 infiltration tests (Table 4). This behavior may reflect subtle concavities in the infiltration curves, possibly due to effects caused by soil sealing, air entrapment, or soil layering (Moret-Fernández et al., 2021; Yilmaz, 2021; Di Prima et al., 2018; Lichner et al., 2013), which are not considered by either model.

Furthermore, additional information about the initial phase of the infiltration process can be obtained from the experimental infiltration rate curve, $i(t)$. Out of the 60 infiltration tests, 24 of them had $i(t)$ curves with convex shapes, and the BEST-WR-3T method showed deviations during the initial infiltration stage of the infiltration process for 23 of the tests (Table 4). This result may explain a large part of the deviation observed between both models and the experimental data. In the second example (Fig. 4, right), BEST-WR-3T has lower Er$_{FIT}$ than BEST-WR-2T, yet the new formulation provided a better estimation of the hydraulic parameters. For this case, the behavior of the infiltration curve (Fig. 5, right) is typical of water-repellent conditions, which the Abou Najm et al. (2021) model is well adapted to represent. However, other tests were less successful. As another example, a break in the cumulative infiltration curve was observed near 700 s in the Berchidda 3F7 test (Fig. 4, left, black arrow). This behavior was also observed in the corresponding infiltration rate curve (Fig. 5, left, black arrow), leading to a convex- followed by a concave-shape. Because the model of Abou Najm (2021) was designed for convex and convex-to-linear behaviors, it

appears to be unable to fit concave-to-convex behaviors that have been observed in soils with fractional wettability (Angulo-Jaramillo et al., 2019).

Despite the deviations frequently seen during the initial infiltration stage, the BEST-WR-3T model fit the latter infiltration stages with good accuracy (Fig. 4, right). This behavior is indicated by the relatively low Er$_{FIT}$ values of between 0.018 and 0.066 when the BEST-WR-3T model had an initial deviation from the experimental data (Table 4). Furthermore, the new three-term formulation shows very good results when the beginning of the experimental curve fits within the expected behavior for water-repellent soils (i.e., increasing infiltration rates through time as water repellency diminishes). In such instances the BEST-WR-3T model provides lower Er$_{FIT}$ values than the BEST-WR-2T method. A second important point is that the BEST-WR-2T approach should only be used on transient-phase data, as the model is not appropriate for steady-state infiltration. Therefore, the correct detection of the transient versus steady-state regimes is necessary to delimit the data set to be used. If the complete dataset is used then the two-term model will deviate (Fig. 4, red dotted lines). Thus, the three-term model has an undeniable advantage since it uses a model that is valid for much longer times.

5. Summary and conclusions

In this study we proposed and validated a new formulation to estimate the hydraulic properties of water-repellent soils. The BEST-WR-3T (adaptation of a three-term approximate expansion for infiltration with an exponential correction factor) model was tested on analytical and

experimental data, and its performance was compared to the previously described BEST-WR-2T (two-term) developed by Di Prima et al. (2021). The new approach showed better ability to estimate hydraulic properties from the analytical data. Indeed, when the water repellency of the soils increased, the BEST-WR-2T method tended to deviate from the target values for K_s and S, with relative errors of 10 % to more than 25 %. The BEST-WR-3T approach resulted in more consistent parameter estimates, particularly in soils with strong repellency, providing relative errors of less than 8 %. However, the results were more mixed when the models were tested on field data. Here, the two methods (BEST-WR-2T and BEST-WR-3T) estimated similar values for S and K_s, with R^2 factors of 0.84 (S) and 0.88 (K_s) between methods. Both models also had some difficulties when the experimental curves presented concavity at the beginning of the infiltration processes, which may be due to analytical features of the two equations used, i.e., Equations (7b) and (8b). This point will be the subject of further studies. In particular, the way to design the correction factor for water repellency has not been appropriately examined and will be the subject of further developments.

Overall, both methods showed very good results for estimating hydraulic properties in water-repellent soils. With that said, the new approach (BEST-WR-3T) was more robust when applied to severely repellent soils within the analytical data set. At the same time, it avoids the need to delimit transient versus steady-state infiltration times, since the three-term expansion was determined to be valid for much longer times than the two-term version. This last point also implies that the BEST-WR-2T approach can suffer error when datasets that include steady-state condition are used to estimate S and K_s. Since soil water repellency often dynamically changes during the course of an infiltration event, it is preferable to perform longer infiltration tests that can capture this range of behavior. We therefore recommend using the new BEST-WR-3T model – especially for soils with strong to severe water repellency – to ensure proper estimation of soil hydraulic properties.

Declaration of Competing Interest

The authors declare that they have no known competing financial interests or personal relationships that could have appeared to influence the work reported in this paper.

Data availability

Data will be made available on request.

Acknowledgment

Appendix

Mathematical development of the three-term formula.

$$i_{\mathrm{WR3T}}(t) = i_{\mathrm{WR2T}}(t) + \frac{1}{6}\left(\beta^2 - \beta + 1\right)\frac{\left(i_{+\infty}^{exp} - AS^2\right)^2}{S}.t^{\frac{1}{2}}(1 - e^{-\alpha_{\mathrm{WR}}t})$$

$$i_{\mathrm{WR3T}}(t) = i_{\mathrm{WR2T}}(t) + \frac{1}{6}\left(\beta^2 - \beta + 1\right)\frac{\left(i_{+\infty}^{exp} - AS^2\right)^2}{S}.t^{\frac{1}{2}} - \frac{1}{6}\left(\beta^2 - \beta + 1\right)\frac{\left(i_{+\infty}^{exp} - AS^2\right)^2}{S}.t^{\frac{1}{2}}.e^{-\alpha_{\mathrm{WR}}t}$$

Integration of $i_{\mathrm{WR3T}}(t)$ in respect to time t leads to:

$$I_{\mathrm{WR_{3T}}}(t) = I_{\mathrm{WR_{2T}}}(t) + \frac{1}{9}\left(\beta^2 - \beta + 1\right)\frac{\left(i_{+\infty}^{exp} - AS^2\right)^2}{S}.t^{\frac{3}{2}} - \frac{1}{6}\left(\beta^2 - \beta + 1\right)\frac{\left(i_{+\infty}^{exp} - AS^2\right)^2}{S}\int_0^t t^{\frac{1}{2}}e^{-\alpha_{\mathrm{WR}}t}dt$$

Using the integration by parts, the upper integral can be rewritten as follow:

	Derivative	Integral
+	$\dfrac{1}{t^{\frac{1}{2}}}$	$e^{-\alpha_{\mathrm{WR}}t}$
−	$\dfrac{\dfrac{1}{t^{-\frac{1}{2}}}}{2}$	$-\dfrac{1}{\alpha_{\mathrm{WR}}}e^{-\alpha_{\mathrm{WR}}t}$

$$\int_0^t t^{\frac{1}{2}}e^{-\alpha_{\mathrm{WR}}t}dt = \left[-\frac{t^{\frac{1}{2}}}{\alpha_{\mathrm{WR}}}e^{-\alpha_{\mathrm{WR}}t}\right]_0^t - \left(-\frac{1}{2\alpha_{\mathrm{WR}}}\right)\int_0^t t^{-\frac{1}{2}}e^{-\alpha_{\mathrm{WR}}t}dt$$

Because $\int_0^t t^{-\frac{1}{2}}e^{-\alpha_{\mathrm{WR}}t}dt = \frac{\sqrt{\pi}}{\sqrt{\alpha_{\mathrm{WR}}}}erf(\sqrt{\alpha_{\mathrm{WR}}t})$, the upper integral can be written using the error function as follows:

$$\int_0^t t^{\frac{1}{2}}e^{-\alpha_{\mathrm{WR}}t}dt = -\frac{t^{\frac{1}{2}}}{\alpha_{\mathrm{WR}}}e^{-\alpha_{\mathrm{WR}}t} + \frac{1}{2\alpha_{\mathrm{WR}}}\frac{\sqrt{\pi}}{\sqrt{\alpha_{\mathrm{WR}}}}\mathrm{erf}(\sqrt{\alpha_{\mathrm{WR}}t})$$

Then the cumulative infiltration for water-repellent soil for three term formulation is adapted as follows:

$$I_{\mathrm{WR_{3T}}}(t) = I_{\mathrm{WR_{2T}}}(t) + \frac{1}{9}\left(\beta^2 - \beta + 1\right)\frac{\left(i_{+\infty}^{exp} - AS^2\right)^2}{S}.t^{\frac{3}{2}} - \frac{1}{6}\left(\beta^2 - \beta + 1\right)\frac{\left(i_{+\infty}^{exp} - AS^2\right)^2}{S}\left\{-\frac{t^{\frac{1}{2}}}{\alpha_{\mathrm{WR}}}e^{-\alpha_{\mathrm{WR}}t} + \frac{\sqrt{\pi}}{2(\alpha_{\mathrm{WR}})^{\frac{3}{2}}}erf(\sqrt{\alpha_{\mathrm{WR}}t})\right\}$$

References

Abou Najm, M.R., Stewart, R.D., Di Prima, S., Lassabatere, L., 2021. A simple correction term to model infiltration in water-repellent soils. Water Resour. Res. 57 https://doi.org/10.1029/2020WR028539.

Angulo-Jaramillo, R., Bagarello, V., Iovino, M., Lassabatere, L., 2016. Saturated Soil Hydraulic Conductivity. In: Angulo-Jaramillo, R., Bagarello, V., Iovino, M., Lassabatere, L. (Eds.), Infiltration Measurements for Soil Hydraulic Characterization. Springer International Publishing, Cham, pp. 43–180.

Angulo-Jaramillo, R., Bagarello, V., Di Prima, S., Gosset, A., Iovino, M., Lassabatere, L., 2019. Beerkan Estimation of Soil Transfer parameters (BEST) across soils and scales. J. Hydrol. 576, 239–261. https://doi.org/10.1016/j.jhydrol.2019.06.007.

Bagarello, V., Iovino, M., Reynolds, W., 1999. Measuring hydraulic conductivity in a cracking clay soil using the Guelph permeameter. Trans. ASAE 42. https://doi.org/10.13031/2013.13276.

Bagarello, V., Di Prima, S., Iovino, M., 2014. Comparing alternative algorithms to analyze the Beerkan infiltration experiment. Soil Sci. Soc. Am. J. 78 (3), 724–736.

Beatty, S.M., Smith, J.E., 2013. Dynamic soil water repellency and infiltration in post-wildfire soils. Geoderma 192, 160–172. https://doi.org/10.1016/j.geoderma.2012.08.012.

Bouwer, H., 1999. Artificial recharge of groundwater: systems, design, and management. Hydraulic Design Handbook. Larry W. Mays, New York. Vol. 24.

Brooks, R.H., Corey, T., 1964. Hydraulic properties of porous media. Hydrol. Paper 3. Colorado State University, Fort Collins.

Burdine, N.T., 1953. Relative permeability calculation from pore size distribution data. Petr. Trans. Am Inst. Min. Metall. Eng. 198, 71–77.

Campbell, S.L., Chancelier, J.-P., Nikoukhah, R., 2010. Modeling and Simulation in Scilab/Scicos with ScicosLab 4.4, 2nd ed. Springer-Verlag, New York.

Carsel, R.F., Parrish, R.S., 1988. Developing joint probability distributions of soil water retention characteristics. Water Resour. Res. 24 (5), 755–769. https://doi.org/10.1029/WR024i005p00755.

Castellini, M., Iovino, M., Pirastru, M., Niedda, M., Bagarello, V., 2016. Use of BEST procedure to assess soil physical quality in the Baratz Lake catchment (Sardinia, Italy). Soil Sci. Soc. Am. J. 80 (3), 742–755. https://doi.org/10.2136/sssaj2015.11.0389.

Cerdà, A., Doerr, S.H., 2007. Soil wettability, runoff and erodibility of major dry-Mediterranean land use types on calcareous soils. Hydrol. Proc. Internat. J. 21 (17), 2325–2336. https://doi.org/10.1002/hyp.6755.

Concialdi, P., Di Prima, S., Bhanderi, H.M., Stewart, R.D., Abou Najm, M.R., Lal Gaur, M., Angulo-Jaramillo, R., Lassabatere, L., 2020. An open-source instrumentation package for intensive soil hydraulic characterization. J. Hydrol. 582, 124492 https://doi.org/10.1016/j.jhydrol.2019.124492.

Di Prima, S., Lassabatere, L., Bagarello, V., Iovino, M., Angulo-Jaramillo, R., 2016. Testing a new automated single ring infiltrometer for Beerkan infiltration experiments. Geoderma 262, 20–34. https://doi.org/10.1016/j.geoderma.2015.08.006.

Di Prima, S., Concialdi, P., Lassabatere, L., Angulo-Jaramillo, R., Pirastru, M., Cerda, A., Keesstra, S., 2018. Laboratory testing of Beerkan infiltration experiments for assessing the role of soil sealing on water infiltration. Catena 167, 373–384. https://doi.org/10.1016/j.catena.2018.05.013.

Di Prima, S., Castellini, M., Abou Najm, M.R., Stewart, R.D., Angulo-Jaramillo, R., Winiarski, T., Lassabatere, L., 2019. Experimental assessment of a new comprehensive model for single ring infiltration data. J. Hydrol. 573, 937–951.

Di Prima, S., Stewart, R.D., Abou Najm, M.R., Roder, R., Giadrossich, F., Campus, S., Angulo-Jaramillo, R., Yilmaz, D., Rogerro, P.P., Pirastru, M., Lassabatere, L., 2021. BEST-WR: an adapted algorithm for the hydraulic characterization of hydrophilic and water-repellent soils. J. Hydrol. 603, 126936 https://doi.org/10.1016/j.jhydrol.2021.126936.

Gette-Bouvarot, M., Volatier, L., Lassabatere, L., Lemoine, D., Simon, L., Delolme, C., Mermillod-Blondin, F., 2015. Ecological engineering approaches to improve hydraulic properties of infiltration basins designed for groundwater recharge. Environ. Sci. Technol. 49 (16), 9936–9944. https://doi.org/10.1021/acs.est.5b01642.

Haverkamp, R., Ross, P.J., Smettem, K.R.J., Parlange, J.Y., 1994. Three-dimensional analysis of infiltration from the disc infiltrometer: 2. Physically based infiltration equation. Water Resour. Res. 30, 2931–2935. https://doi.org/10.1029/94WR01788.

Lassabatère, L., Angulo-Jaramillo, R., Soria Ugalde, J.M., Cuenca, R., Braud, I., Haverkamp, R., 2006. Beerkan estimation of soil transfer parameters through infiltration experiments—BEST. Soil Sci. Soc. Am. J. 70 (2), 521–532.

Lassabatere, L., Di Prima, S., Angulo-Jaramillo, R., Keesstra, S., Salesa, D., 2019. Beerkan multi-runs for characterizing water infiltration and spatial variability of soil hydraulic properties across scales. Hydrol. Sci. J. 64, 165–178. https://doi.org/10.1080/02626667.2018.1560448.

Lichner, L., Hallett, P.D., Drongová, Z., Czachor, H., Kovacik, L., Mataix-Solera, J., Homolák, M., 2013. Algae influence the hydrophysical parameters of a sandy soil. CATENA 108, 58–68. https://doi.org/10.1016/j.catena.2012.02.016.

Minasny, B., McBratney, A.B., 2007. Estimating the Water Retention Shape Parameter from Sand and Clay Content. Soil Sci. Soc. Am. J. 71, 1105–1110. https://doi.org/10.2136/sssaj2006.0298N.

Moret-Fernández, D., Latorre, B., López, M.V., Pueyo, Y., Lassabatere, L., Angulo-Jaramilo, R., Rahmati, M., Torma, J., Nicolau, J.M., 2020. Three-and four-term approximate expansions of the Haverkamp formulation to estimate soil hydraulic properties from disc infiltrometer measurements. Hydrol. Process. 34 (26), 5543–5556. https://doi.org/10.1002/hyp.13966.

Moret-Fernández, D., Latorre, B., Lassabatere, L., Di Prima, S., Castellini, M., Yilmaz, D., Angulo-Jaramilo, R., 2021. Sequential infiltration analysis of infiltration curves measured with disc infiltrometer in layered soils. J. Hydrol. 600, 126542 https://doi.org/10.1016/j.jhydrol.2021.126542.

Rahmati, M., Latorre, B., Lassabatere, L., Angulo-Jaramillo, R., Moret-Fernández, D., 2019. The relevance of Philip theory to Haverkamp quasi-exact implicit analytical formulation and its uses to predict soil hydraulic properties. J. Hydrol. 570, 816–826. https://doi.org/10.1016/j.jhydrol.2019.01.038.

Rahmati, M., Vanderborght, J., Šimunek, J., Vrugt, J.A., Moret-Fernández, D., Latorre, B., Lassabatere, L., Vereecken, H., 2020. Characteristic time and its usage for improving estimation of the soil sorptivity and saturated hydraulic conductivity from one-dimensional infiltration experiments. Vadose Zone J. 19, e20068.

Seddaiu, G., Bagella, S., Pulina, A., Cappai, C., Salis, L., Rossetti, I., Lay, R., Rogerro, P.P., 2018. Mediterranean cork oak wooded grasslands: synergies and trade-offs between plant diversity, pasture production and soil carbon. Agrofor. Syst. 92 (4), 893–908. https://doi.org/10.1007/s10457-018-0225-7.

van Genuchten, M.T., 1980. A closed-form equation for predicting the hydraulic conductivity of unsaturated soils. Soil Sci. Soc. Am. J. 44 (5), 892–898.

Wessel, A.T., 1988. On using the effective contact angle and the water drop penetration time for classification of water repellency in dune soils. Earth Surf. Proc. Land. 13 (6), 555–561. https://doi.org/10.1002/esp.3290130609.

Yilmaz, D., 2021. Alternative α* parameter estimation for simplified Beerkan infiltration method to estimate soil saturated hydraulic conductivity. Eurasian Soil Science 50, 1049–1058. https://doi.org/10.1134/S1064229321070140.

Yilmaz, D., Lassabatere, L., Angulo-Jaramillo, R., Deneele, D., Legret, M., 2010. Hydrodynamic Characterization of Basic Oxygen Furnace Slag through an Adapted BEST Method. Vadose Zone J. 9, 107. https://doi.org/10.2136/vzj2009.0039.

Yilmaz, D., Bouarafa, S., Peyneau, P.E., Angulo-Jaramillo, R., Lassabatere, L., 2019. Assessment of hydraulic properties of technosols using Beerkan and multiple tension disc infiltration methods. Eur. J. Soil Sci. 70, 1049–1062. https://doi.org/10.1111/ejss.12791.